Does Urban Landscape Composition and Configuration Regulate Heat-Related Health Risk? A Spatial Regression-Based Study in World's Dense City Delhi, India.

Suvamoy Pramanik[1*]; Milap Punia[2]; Saurav Chakraborty[3]

1. School of Social Sciences (SSS), Jawaharlal Nehru University, New Delhi – 110067, India
2. School of Social Sciences (SSS), Jawaharlal Nehru University, New Delhi – 110067, India.
3. Department of Geography, Presidency University, 86/1 College Street Road, Kolkata, West Bengal – 700073, India.

***Corresponding Author**

Suvamoy Pramanik

R.N – 250 (Old), Brahmaputra Hostel, JNU New Campus, New Delhi – 110067, India

Phone: +91 9002761870

Email: suvamoy.vu@gmail.com; suvamo60_ssf@jnu.ac.in.

ORCID ID: https://orcid.org/0000-0003-1350-5246

Does Urban Landscape Composition and Configuration Regulate Heat-Related Health Risk? A Spatial Regression-Based Study in World's Dense City Delhi, India.

Abstract:

Urbanization induced land use land cover (LULC) changes intensify the urban heat island effects. It magnifies the risk of urban dwellers and sometimes causes the loss of human life, defined as heat-related health risk (HRHR). Hence, urban LULC planning plays a crucial role. Present study analyses the impact of composition and configuration of urban LULC defined as urban landscape metric (ULM) on HRHR in Delhi at the ward level. Firstly, the HRHR is measured by using satellite thermal and other digital data. Then, measured HRHR is validated by conducting a rapid field survey. Thirdly, ULM measured at ward level using Fragstat 4 software. Finally, both, HRHR and ULM linked with bi-variate Moran's I and impacts of ULM are assessed using ordinary least square (OLS) and spatial error (SE) regression. The result indicates the high risk is found as clustered in north-east, central and middle of south-west Delhi. Built-up density intensifies HRHR and abundance of vegetation reduce it; however, it is not similar for all vegetation patches. Larger vegetation patches surrounded by dense built-up might not able to reduce the risk as much as a large vegetation patch could in other regions. Findings can be helpful for heat resilient city planning.

Keywords: *Urban Heat Island; Heat-Related Health Risk (HRHR); Urban Landscape Metrics (ULM); Local Indicators of Spatial Autocorrelation (LISA); Spatial Error (SE) Regression; NCT-Delhi.*

1. Introduction:

Rapid urbanization continuously intensifying the effects of urban heat island (i.e., comparatively higher land surface or air temperature in urban areas than surrounding rural areas during day or night) around the world (Chakraborty and Lee, 2019; Patz et al., 2005) and threatens the human health and wellbeing (Harlan et al., 2006). Globally, it often caused the most significant casualty than other natural disasters (Gabriel and Endlicher, 2011). For instance, in the United States, more people were died by city heat than by other natural disasters(Cunningham, 2018). This scenario remains similar for Europe, Australia and China (Zhang et al., 2019). Indian metropolitan cities are also getting affected by a severe heatwave in the recent past. Approximately 2500 people had died in multiple regions of Hyderabad (46°C) in Andhra Pradesh (PTI, 2015), Allahabad (47.8°C) (The Guardian, 2016), and Delhi (45.5°C) in northern India (Thakur, 2017). Rapid urbanization enhanced UHI and reduces the diurnal temperature range (DTR) in the densified metropolitan area in Delhi (Mohan and Kandya, 2015). The heat-related mortality rate is very high in Delhi than London and Sao Palo though it depends on the age group of people (Azhar et al., 2017; Mohan and Kandya, 2015). Global prediction indicated heat-related mortality would increase to around 257% by the end of the 2050s concerning its current annual base of 2000 deaths (Hajat et al., 2005). Parallelly, 90% of the world population will live in cities in the future (Nations, 2018). Therefore, it is crucial to assess relationships between the heat-related health risk (HRHR) and urbanization at the city scale for a sustainable city plan (Johnson et al., 2009; Mushore et al., 2018; Tomlinson et al., 2011).

HRHR can be defined as the potential health risk of physiologically and socio-economically vulnerable people due to high heat in cities. These include infants, elderly, physically challenged people, poor and marginalized people, outdoor workers, and slum dwellers (WHO, 2018). Besides, potential HRHR includes heat cramps, heat exhaustion,

heatstroke, hyperthermia, and sometimes death also occurred (Mavalankar et al., 2013; WHO, 2018). It worsens the patient's condition with other co-morbidity (i.e., cardiovascular, raspatory, cerebrovascular disease, and diabetes). However, along with the physical condition of health, mental, and behavioral conditions can also be affected by extreme heat (Mavalankar et al., 2013; WHO, 2018).

High heat can be regulated by suitable land use land cover (LULC) design and planning. However, we need a clear understanding of the relation between LULC and heat (Li et al., 2011). Urbanization, world-wise responsible for the rapid transformation of the natural earth surface (i.e., vegetation, water, soil) to the irreversible artificial surface (i.e., cemented, concreted). This alteration causes modification of thermal inertia, hydrological and thermal balances, and overall thermal environment of the city (Suvamoy Pramanik and Punia, 2019). Previously these interactions were well documented through LST and LULC linkages (Mohammad et al., 2019; Mohan and Kandya, 2015; Sultana and Satyanarayana, 2018). But, in recent days, 'landscape ecology' based analysis, i.e., landscape metrics, are getting popular. 'Landscape Metrics' is defined as composition and configuration or pattern of the land use classes within a unit of the area (Li et al., 2011; Suvamoy Pramanik and Punia, 2019; Zhou et al., 2020, 2011). It is getting popular in UHI studies as it focuses on functional aspects of LULC – UHI relation with practical implication on LULC designing. For instance, the proper arrangement of green spaces could increase the cooling effects (heat sink), and dense built-up could reduce cooling effects (heat sources) (Pramanik and Punia, 2019). However, there are no ideal landscape designs as it much depends on geographical location, seasonality, and window of the analysis (Yue et al., 2019). Hence, extensive research needs to understand the effects of urban landscape metrics (ULM) and UHI. Here, we, for the first time, assessed the relationship between HRHR with ULM for a better understanding of heat resilient landscape design.

2. Literature Review:

2.1. Conceptual Background for health risk assessment:

According to Crichton (1999), the risk is the probability or chances of loss and function of exposure, vulnerability, and hazard. All component of this risk framework has an equal and significant influence on Risk assessment strategies (Fig.-1).

$$Risk = f(Exposure \times Vulnerability \times Hazard) \quad (1)$$

Buscail et al., 2012 argue that all elements of risk assessments have to be active and should give equal importance for successful appraisal of risk. *Exposure* is an association of such an aspect upon which risk may happen, like population density (Buscail et al., 2012). Besides, the *vulnerability* of a society indicates the demographic, social, and economic crisis. It can be occurred due to a lack of proper socio-economic infrastructure and a community unable to cope up with the hazard situation, for instance, socio-economic status, extreme age, etc. (Johnson et al., 2012). Also, the *hazard* is the extreme climatic events (depending on the perspective of research, it varies from climatic to the technological) and due to which this particular section of society could be vulnerable, like extreme heat events (Estoque et al., 2020). The combination of all these three creates the final health risk (Tomlinson et al., 2011).

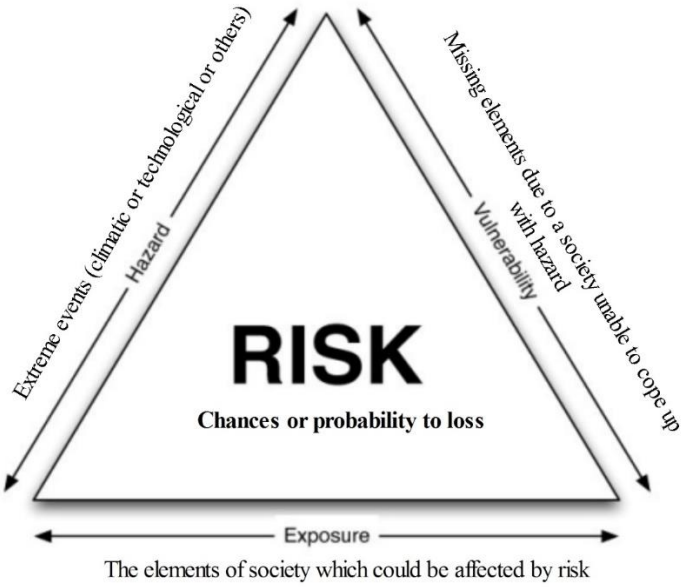

Fig. 1. Conceptual framework of risk estimation after Crichton's (1999) risk triangle.

2.2. Emerging dimension of UHI studies – HRHR and geo-spatial perspective:

There are several studies which are documented the effects of heatwaves on human health like excess mortality in the UK during the 1995 heat wave(Rooney et al., 1998); USA (Curriero et al., 2002; O'Neill et al., 2003); Europe during 2003 (Fouillet et al., 2006; Garssen et al., 2005); and in Australia (Yaron and Niermeyer, 2004) etc. Mapping of spatial variation of heat exposure and risk at different scales was the primary interest of previous researchers (Buscail et al., 2012; Johnson et al., 2009; Mushore et al., 2018; Tomlinson et al., 2011). For instance, high population density always associated with elevated LST, which implies more densification causing UHI effects (Mallick and Rahman, 2012; Tomlinson et al., 2011). Moreover, demographically, the spatial pattern of most susceptible age groups (i.e., children below 5 Yrs. age and elder above 60+ Yrs.) also play a crucial aspect for high HRHR (Vandentorren et al., 2006; Yaron and Niermeyer, 2004). Additionally, the behavioral pattern of human beings also modifies the heat-mortality linkage. Like, higher education level of the

people associated with higher death rates during extreme heat (O'Neill et al., 2003). Single households (i.e., reside alone, never married, widow, and divorced) were found to be more risk-prone compared to others during heat waves (Fouillet et al., 2006). In developing countries, over migration of low & medium-income people to the city caused informalisation. Crisis of suitable housing, basic amenities, and sanitation, etc., (Singh and Grover, 2015) added more people to fragile, susceptible, and vulnerable sections of society (Azhar et al., 2017; Wang et al., 2019). However, previous scholars mainly focused on the social or human dimension of risk assessment (Cutter et al., 2003).

Recently, Remote Sensing (RS) and Geographical Information System (GIS) can successfully assess the HRHR (Buscail et al., 2012; Tomlinson et al., 2011) by combining both social and bio-physical indices (Mushore et al., 2018). It uses multiple layers of risk assessment and gives generalized output at various scales. These layers include MODIS & Landsat derived LST, census-based socio-economic & demographic variables (Johnson et al., 2012), building architecture (Mavrogianni et al., 2011), and RS based biophysical variables (i.e., NDVI, NDWI)(Mushore et al., 2018). Among all, bio-physical indicators are newly introduced for incorporating ecological aspects in the HRHR assessment. NDVI & NDWI, for example, used as a proxy of vegetation abundance and moisture content, respectively (Mushore et al., 2018) and found as heat reducer in previous studies (Chakraborti et al., 2019; Suvamoy Pramanik and Punia, 2019). Besides, the most recent study by Zhang et al., (2019), identified the essential need for incorporating night time LST and air-quality in heat risk methods for their effective synergies with mortality and morbidity. Hence, the integration of the geo-spatial aspect in HRHR holds a promising potentiality.

2.3. Integrating ULM with HRHR:

In previous studies, several heat mitigation strategies intended to support to build the green city for a heat resilient city planning (Yu et al., 2020). Globally, this argument, although justified by the various empirical and qualitative studies (Mohammad et al., 2019; Sultana and Satyanarayana, 2018; Vyas et al., 2014; Zhou and Cao, 2020). These studies can be grouped in two broad categories—the first group are linked with the bio-physical indicators through inferential statistics, and second groups which are trying to find interrelation between UHI and LULC through descriptive statistics or landscape patterns or metric based analysis (Yue et al., 2019). Numbers studies identified spatial patterns of LULC effectively control UHI in a given environment as it the best adaptive tools for UHI mitigation (Lindley et al., 2007). However, the debate whether 'dense or compact city' or 'sprawling city' enhance the UHI still exists in the literature (Stone et al., 2010; Yue et al., 2019). Tomlinson et al., (2011) found densification is more likely to capture the heat compare to the non-urban due to high thermal inertia of impervious surface. Contrarily, Stone et al., (2010) found sprawling city rapidly altered the surface's thermal and hydrological properties, hence prominent the UHI effects. So, this contradiction of arguments in the literature highlights the complexity in UHI studies, which undoubtedly seek the city-specific assessment of LULC and UHI context. In parallel, as high UHI creates high risk (Buscail et al., 2012), relation of HRHR with 'landscape Metric' also seek similar attention. Because, Mushore et al., (2018); and Tomlinson et al., (2011) found compact city is high vulnerable than sprawling city and vice-versa. However, their arguments were lacking of proper statistical evidence. The present study investigate this research gap.

The scientific model of health risk assessment can be considered as a starting point of the risk-governance framework for resilient climatic policies of cities (Zhang et al., 2019) despite its complex and multidimensional nature (Mavrogianni et al., 2011). However, most of the HRHR assessment only done in developed countries, although, cities in developing nations

are severely affected by heat stress in the recent past and lacking comprehensive heat risk assessment framework (Azhar et al., 2017; Mushore et al., 2018; Wang et al., 2019; Zhang et al., 2019) This study is unique from following three aspects – i) for the first time mapping of HRHR in NCT Delhi at the local scale by incorporating social, economic, biophysical and GHG CO2 emission and build a comprehensive risk index; ii) measurement of spatial correlation of ULM of built-up and green space with HRHR and iii) quantification of the spatial influence of ULM on HRHR using spatial regression approach.

3. Materials and Methodology:

3.1. Study area:

National capital territory – Delhi is one of the largest and dense metropolitan regions situated in the north of India. It is located at 28°-24'-17" N, 76°-50'- 24" E to 28°-53'-00" N, 77°-20'- 37" E (Fig. 2). Delhi is spread over an area of 1484 km^2 and has a population of 16.78 million (Government of India, 2011). The population density is 11297 Person/ km^2, the highest in the country and second in the world. The weather is most extreme. The summer (April-July) temperature ranges from 25°C to 45°C and the winter (December- January) ranges from 22°C to 5°C. Delhi also faced extreme heatwaves in summer, and temperature some-times crossed 5°C limits than the normality (Thakur, 2017).

3.2. Database and Methods:

Remotely sensed data, census information, and some alternative data (i.e., gridded demographic data, GHG CO_2, etc.) have been used for the analysis. The details explanation and reasons for using the database has been describing in table 1

NDVI and NDBI are calculated using methods described in Chen et al., 2006. Then all data like NDVI, NDBI, GPW population characteristics (i.e., count, density, age group) and

MODIS Aqua (MYD11A1) average summer seasons night LST are extracted within the CW using spatial analyst tools of ArcGIS10.4. Next, all the data are normalized in 0 to1 scale, where 0 & 1 indicates the minimum and maximum vulnerability, respectively. For NDVI, below 0 to -1 fixed as 0 because it is water body and NDVI value 0 to +1 normalized reciprocally – i.e., 0 means high vulnerable, and 1 means less (Mushore et al., 2018).

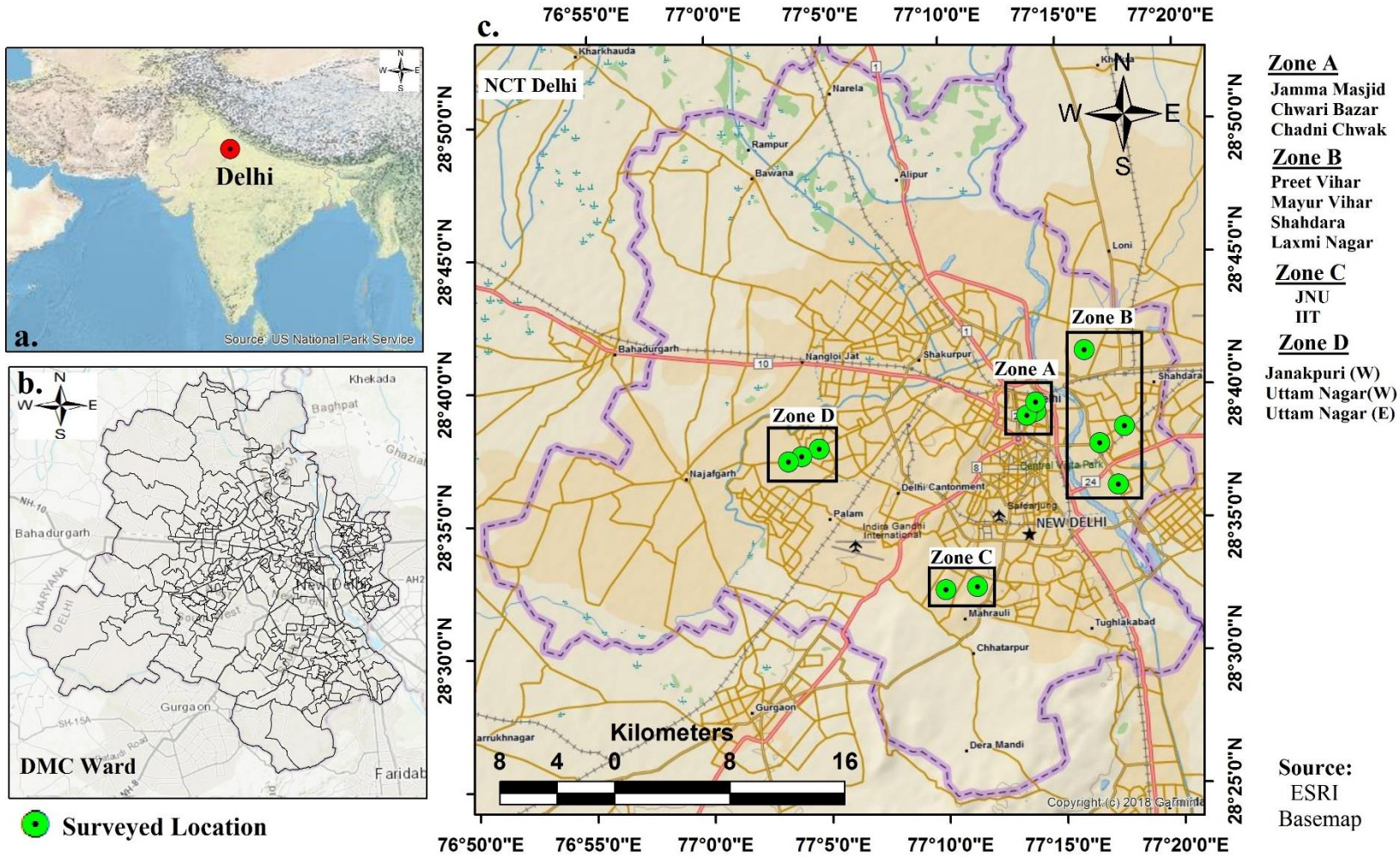

Fig. 2. Location map of the study area.

Table 1. Details of the database used for risk assessment.

Purpose	Sub Layers		Layer's property	Variables	Explanation	Sources
Risk assessment after Crichton's risk assessment framework.	Exposure		Population Distribution	GPW- v4.10, Population count	It is the layer upon which risk may happen, or If there are no people, there may not be any health risk (Doxsey-Whitfield et al., 2015)	(CIESIN, 2018)
	Vulnerability	Social	Population Density	GPW- v4.10, Population density, and demographic age data	Highly dense population area is more prone to heat health risk because of congested environment restrict the natural cooling process	(CIESIN, 2018)
			Child Population (0-4 Yr.)		Age-sensitive or vulnerable populations, i.e., child and older people, are most susceptible because they are dependent upon others and physiologically susceptible.	
			Aged Population (65+ Yr.)			
			Household condition	Percentage of good household (HH)	It is used here as a proxy of the economic status of a household. CoI defines good HH as those houses which do not require any repairs and in good condition.	Census of India (CoI), 2011
			Drinking water	Drinking water within the premises	It is used as a proxy of basic amenities for immediate remedies of heat risk. According to CoI, premises means buildings along with land or commonplaces attached to it (Azhar et al., 2017).	Census of India, 2011

			Fossil fuel emission database	Gridded(1km*1km) CO2 emission data	CO2 emission is a proxy of anthropogenic heat release, especially from transport, industrial and residential sectors. Because it has a profoundly positive correlation with LST (Oda et al., 2018)	ODIAC, 2016
		Bio-physical	Vegetation abundance	NDVI	Less vegetation abundance makes a high probability of risk. (Mushore et al., 2018)	Landsat 8 (OLI), 2017
			Built-up density as a proxy	NDBI	The imperviousness of land surface increases thermal stress. (Mushore et al., 2018)	
	Hazard		Summer night LST	LST	Average night LST of summer seasons taken as an example of the hazard layer. Because the previous study found UHI intensified during the night in Delhi (Chakraborty and Lee, 2019).	MODIS LST (MYD11A2)
Urban landscape metrics (ULM)			Landscape metrics of two broad classes – built-up and urban greenery	PLAND, LPI, PD, LSI	How urban land use pattern affects the health risk scenario was assessed to understand better and plan.	Landsat 8 (OLI), 2017

3.2.1. Mapping of HRHR:

HRHR is mapped using a weighted linear sum (WLS) function, which able to integrate different layers of information into a single layer with appropriate weight. It is a numerical value used in the analysis to specify the relative importance of any variable than others. There are two weighting systems available, i.e., equal and different weight (Buscail et al., 2012; Tomlinson et al., 2011). Different weight system often leads to subjective manipulation in the risk assessment procedure (Tomlinson et al., 2011); hence uniform weight system has been adopted in this study. Details of the equal weight system adopted in this study were described in (Mushore et al., 2018).

3.2.2. LULC classification and derivation of ULM:

LULC map was prepared from Landsat 8 OLI image of 6th April 2017 (Path/Row – 146/40). Before applying the classification scheme, Fast Line-of-Sight Atmospheric Analysis of Hypercubes (FLAASH) module for atmospheric correction was applied in band 2 to 7. LULC has been prepared using Maximum likelihood supervised classification scheme. We considered five LULC classes, i.e., built-up areas, agricultural field, bare land or rocky exposed land, urban greenery, and water bodies. Accuracy of the classified map was done using Kappa statistics (k=87.67) **(Supplementary 1 & 2)**.

ULM of two LULC classes, i.e., built-up and greenery, were calculated while keeping CW as analytical units. We calculated four metrics, i.e., percentage of landscape (PLAND); patch density (PD); largest patch index (LPI), and landscape shape index (LSI), to represent proportion, fragmentation, centrality and shape complexity respectively. All ULM were calculated using Fragstat 4.2 (Mcgarigal, 2012) and explained in Table 2.

Table 2. Explanation of selected basic urban form of built-up and green space.

Name of the ULM	Explanation	Formula	Unit	The syntax used in the study
Percentage of greenspace (PLAND)	Percent of the area of BU/GS covered in a census tract or ward	$Pi = \frac{\sum_{j=1}^{n} a_{ij}}{A}(100)$	Percent	PLAND_B; PLAND_V
Patch Density (PD)	Number of patches of BU/GS in a total landscape area	$PD = \frac{n}{A}$	Number / m2	PD_B; PD_V
Largest Patch Index (LPI)	Area (m^2) of the largest patch of BU/GS divided by total landscape area (m^2). It is multiplied by 100 to convert it into the percentage	$LPI = \frac{\max(aj)_{j=1}^{a}}{A}(100)$	Percent	LPI_B; LPI_V
Landscape shape index (LSI)	The total perimeter of BU/GS divided by the minimum perimeter of green space edge possibly for maximum aggregated class	$LSI = \frac{E}{minE}$		LSI_B; LSI_V
Where Pi = proportion of the landscape occupied by patch types i (green space); a_{ij} = area (m2) of patch ij. A = total landscape area (m2); n = number of patches. E = total length of the perimeter of green spaces includes all landscape boundary and background edge segments of greenspace; E_{min} = minimum total length of edge or perimeter of green space; BU = Built-up; GS = Green space				_B and _V denotes for built-up and vegetation respectively

3.2.3. Univariate and bivariate Local Indicator of Spatial Autocorrelation (LISA):

Univariate - LISA was applied to HRHR and ULM to show individual spatial clustered and outlier **(Sup. 3& 4)**. It is the geographical version of standard autocorrelation, represent as follows -

$$I = \frac{N\sum_{i=1}^{n}\sum_{j=1}^{n} w_{ij}(x_i - \bar{x})(x_j - \bar{x})}{(\sum_{i=1}^{n}\sum_{j=1}^{n} w_{ij})\sum_{i=1}^{n}(x_i - \bar{x})^2}. \quad (2)$$

Where, N is the number of observations (points or polygons); X_i is the variable value at location *i*; X_j is the variable value at location j; W_{ij} is a weight indexing location of i relative to j; $\bar{x}$ is the mean of all observational values. Moran's, *I* vary and ranging from +1 to -1. +1 indicate strong positive spatial auto-correlation, 0 indicate perfect random, and -1 suggest that strong negative spatial autocorrelation (Moran, 1950).

Bivariate Moran's *I* was applied to explore the spatial correlation between HRHR and ULM, where HRHR and ULM considered as the dependent and independent variables, respectively. It has two components – clustered (i.e., High-High & Low-Low) and outlier (i.e., High-Low & Low-High). 'High-High' clustered means high value of risk is spatially correlated with a high value of ULM, which is spatially lagged (like PLAND_B), and 'Low-Low' indicates a low value of risk spatially associated with lagged low value of ULM. The outlier indicates when the previous scenario interchanged. Bi-variate LISA was calculated using equation (3) after (Anselin et al., 2006).

$$I = \frac{x_i - \bar{x}}{\sum_i (x_i - \bar{x})^2} \sum_j w_{ij}(x_j - \bar{x}) \quad (3)$$

Where x_i and x_j are the value of the attributes x at location i and j, $\bar{x}$ is the average value of the census tract, w_{ij} is the spatial weight matrix.

3.2.4. Ordinary Least Square (OLS) and Spatial Error Regression (SER):

The simplest form of the linear regression, i.e., OLS, is based on four fundamental criteria – a) responsible variable is a linear function of explanatory variables; b) independent nature of the error or residual term (e); c) normality of residual (e); and d) homo-scedasticity of error terms (e) (Du et al., 2016). This model can describe as follows ---

$$Y_i = a + \beta_1 X_1 + \beta_2 X_2 + \cdots \ldots \ldots \ldots \ldots + \beta_n X_n + \varepsilon \quad (4)$$

Where, Y_i is predicted variable; a is constant or height from the base; $(\beta_1 \ldots\ldots \beta_n)$ is coefficient value or slope; $(X_1 \ldots\ldots X_n)$is an explanatory variable, and ε is error terms. In this study, OLS has been used to see preliminary effects ULM upon HRHR. However, major loopholes of the OLS model are, it couldn't encounter spatial dependency of the dependent variable (y), and spatial auto-correlation of residual or error terms (e), which leads to biased estimation and model may not have practical efficiency (Anselin et al., 2006). The spatial error (SE) regression model has been adopted to avoid this bias.

The assumption for SE regression models or spatial error dependence is spatial autocorrelation process occurred in the error terms (ε) and entered explanatory variables that are not able to fully explained the spatial effects. It can be expressed as

$$y = \beta X + \lambda W\mu + \varepsilon \quad (5)$$

Where $W\mu$ is (N × 1) vector of spatially lagged error, λ is a spatial autoregressive coefficient. For generating the spatial weights, first-order queen's contiguity method was applied upon the wards, the spatial units for the analysis, and neighbor are defined by the immediate adjacent wards of target wards. The comparison of the model has been made using Moran's I value of residuals F statistics and AIC value.

4. Validation:

Validation of the result is a very crucial aspect of risk assessment study (Reid et al., 2012). We conducted a rapid filed survey of random respondents during March-April 2018 using a semi-structured questionnaire while targeting different risk zones (Fig – 6 & 11). Four zones, i.e., A, B, C, and D, assumed based on the surveyed location (Fig.- 2). Where zones A, B, D were in very high, and high and C was in medium HRHR zone. The questionnaire had two parts – basic awareness was assessed by a 5-point Likert scale (Table 3) and an open-ended view on health issues due to heats.

Table 3. Lists of questions asked to respondents

Questions	Likert Score
1. Do you aware of temperature rising?	1. Completely Yes 2. So Yes 3. Neither Yes nor No 4. So No 5.Completely No * For question 9, 1 = Very Poor 5 = Very Good
2. Do you realize the impact of temperature rise?	
3. Do you feel that temperature is rising in the last 3-5 years?	
4. Do you understand the causes of temperature rise?	
5. Do you consider that urbanization and industrialization are the reasons of temperature rising?	
6. Do you suffer from health illness due to the temperature rising?	
7. Do you give/ receive any support to/ from others? (Neighbourhood, NGOs, Social groups).	
8. Do you get any support from the government? i.e., proper forecasting, caution, warning messages, etc.	
9. How many scores do you want to give about health risks in the summer season in Delhi?	

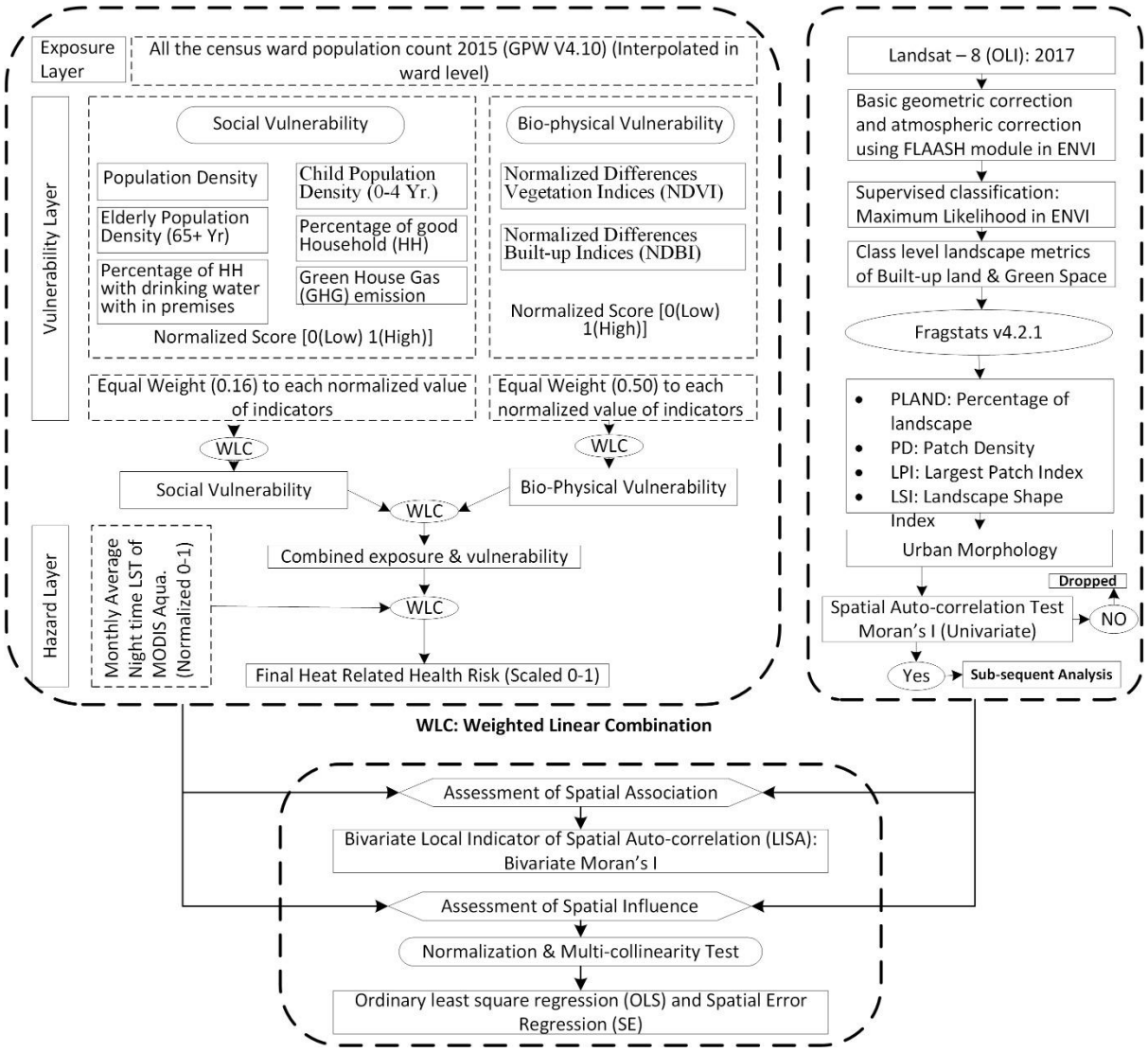

Fig. 3. Details methodological flow chart of assessment of HRHR & ULM and their relationship.

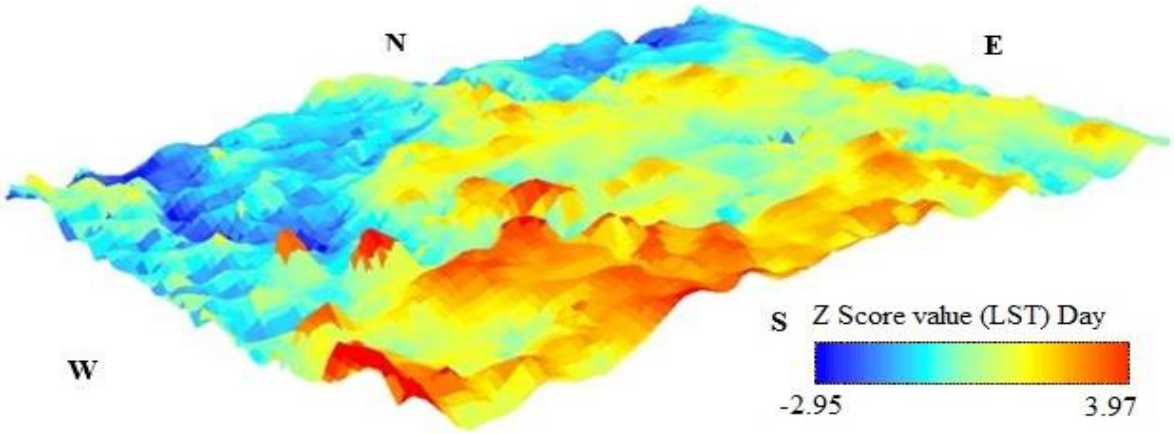

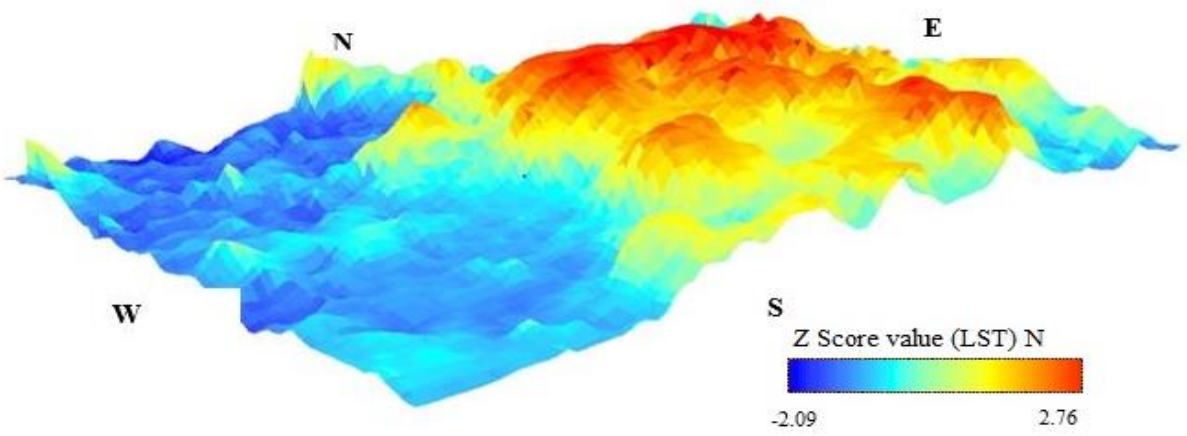

Fig. 4. 3-D representation of average suffer day (upper)/ night (lower) land surface temperature over Delhi and its surroundings.

4. Result:

4.1 Estimation of HRHR:

The demographic characteristics, i.e., population density, child, and aged population density, were consistent with a similar spatial pattern, i.e., high in the North-East (NE) and Central (CL) part of Delhi. GHG emission also follows the same pattern of population density because of emission from anthropological sources, i.e., transport, mixed residential/commercial, and industrials sectors. Percentage of good households, as well as treated tap water within premises, have similar spatial distribution i.e., comparatively good in the city centre but low in the periphery regions of Delhi.

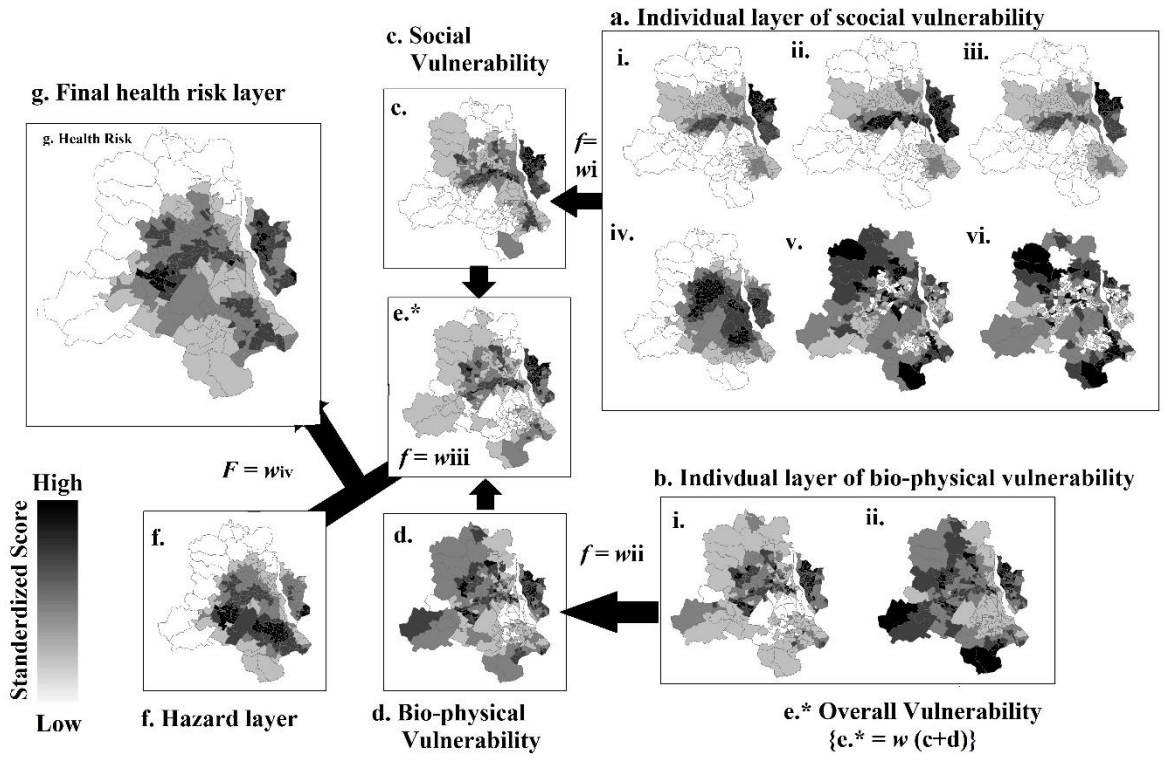

Fig. 5. Step by step HRHR assessment procedure. a) different layers of social vulnerability; b) layers of bio-physical vulnerability; c) combined social vulnerability; d) combined bio-physical vulnerability; e) combined overall vulnerability; f) hazard layer; g) Final HRHR with the combination of hazard and combined vulnerability.

The composite social vulnerability was maximum in NE of Delhi and followed narrow stripe from West (W) to East(E). Some census tracts of South-West (SW) Delhi also showed high socio-economical vulnerability. The reason is that people are located in a comparatively dense, informal, and excluded section of society (Kumari and Punia, 2017). Bio-physical vulnerability also found to be very high in the NE and Central-West (CW) parts of Delhi (Fig. 5.b). Overall vulnerability shows a similar spatial pattern (i.e., NE, Central Delhi) with social and biophysical vulnerability and indicates high levels of HRHR in these areas (Fig 5.c).

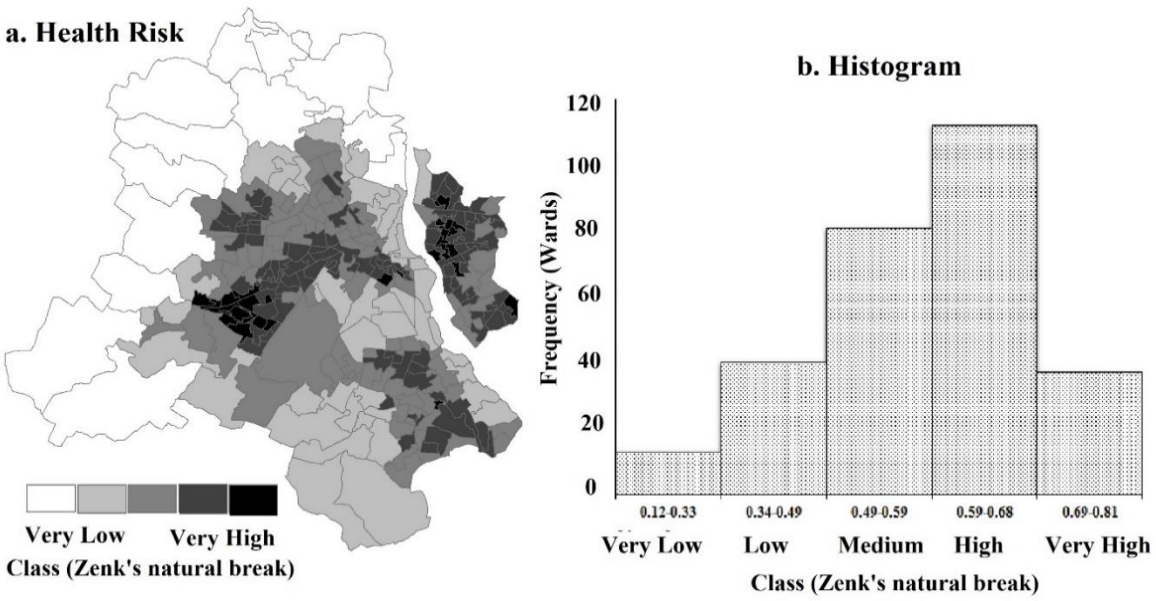

Fig. 6. The final map of HRHR; a) spatial pattern of HRHR in Delhi; b) class wise risk distribution of the number of wards (Total number DMC wards is 272, Census of India, 2011.

However, the total number of polygons is 282, which includes NDMC and DCB part). However, final HRHR map represented that very high-risk zone (0.69 – 0.81) was mainly concentrated in three pockets like in NE, SW and form a straight stretch in the west of central Delhi which is surrounded by high (0.59 - 0.68) and moderate risk (0.49 – 0.59) zones. Low (0.34 – 0.49) and very low (0.12 – 0.33) risk mainly found along North, NW, and SW of Delhi (Fig. 6), along the western periphery of NCT Delhi.

4.2. Spatial associations between ULM and HRHR:

Bivariate LISA is taken into consideration for estimating of spatial association between HRHR and ULM. Fig.7 indicates PLAND_B and LPI_B form HH clustered in a similar pattern, i.e., highly concentrated in North-East, middle of South-West Delhi. It means dense, and compact urban areas are more risk-prone to during night in summer seasons. Whereas, LL clustered is mainly seen in periphery regions of Delhi. Surprisingly PD_B and LSI_B didn't form any cluster as they appeared as outliers that means low-risk value surrounded by the high

value of PD_B and LSI_B (LH) or vice-versa (HL). Bivariate LISA between ULM of greenery and risk indicates (Fig 8) PLAND_V and LPI_V follow a similar pattern as they formed 'L-H' outlier across the southern portion of Delhi, which proved the low value of risk due to high vegetation abundance. In contrast, 'H-L' outlier found in north-eastern Delhi, means high risk due to low vegetation abundance. Surprisingly we found an 'H-H' clustered in SE Delhi, may due to CW with elevated HRHR surrounded by the larger vegetation patch. In the case of LSI_V, the 'L-H' outlier has been formed along the western periphery of Delhi.

Moran's I statistics and scatters plot depicted that PLAND_B and LPI_B (Moran's I = 0.54 & 0.54 respectively) positively associated with risk, whereas the relationship with PD_B and LSI_B is negative. It is indicating dense, and compact urban areas are more risk-prone to during night in summer seasons. In contrast, risk reduces accordingly with the fragmented built-up area. In contrast, every form of vegetation, i.e., PLAND_V; LPI_V; LSI_V, are negatively correlated with the risk, indicating, form urban vegetation is significantly reducing HRHR. Though, very low *Moran's I* for PD_V (i.e., 0.10) means fragmented vegetation couldn't be able to reduce risk significantly. (Fig. 7 & 8)

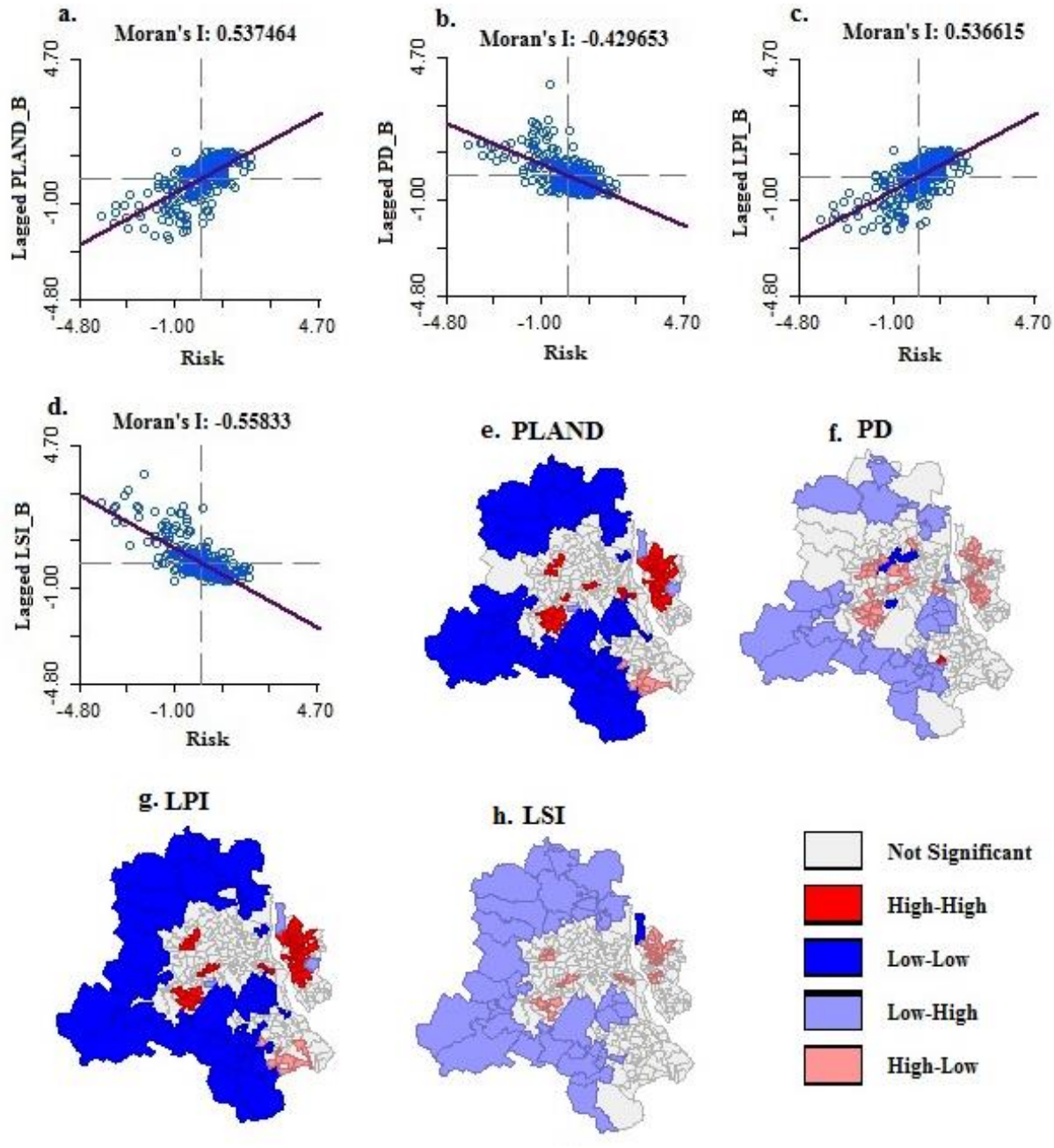

Fig. 7. Bi-variate Moran's I scatter plot between risk and built-up form- a) risk vs. lagged PLAND; b) risk vs. lagged PD; c) risk vs. lagged LPI; d) risk vs. lagged LSI; and bi-

variate LISA clustered map- e) risk vs. PLAND; f) risk vs. PD; g) risk vs, LPI; h) risk vs LSI.

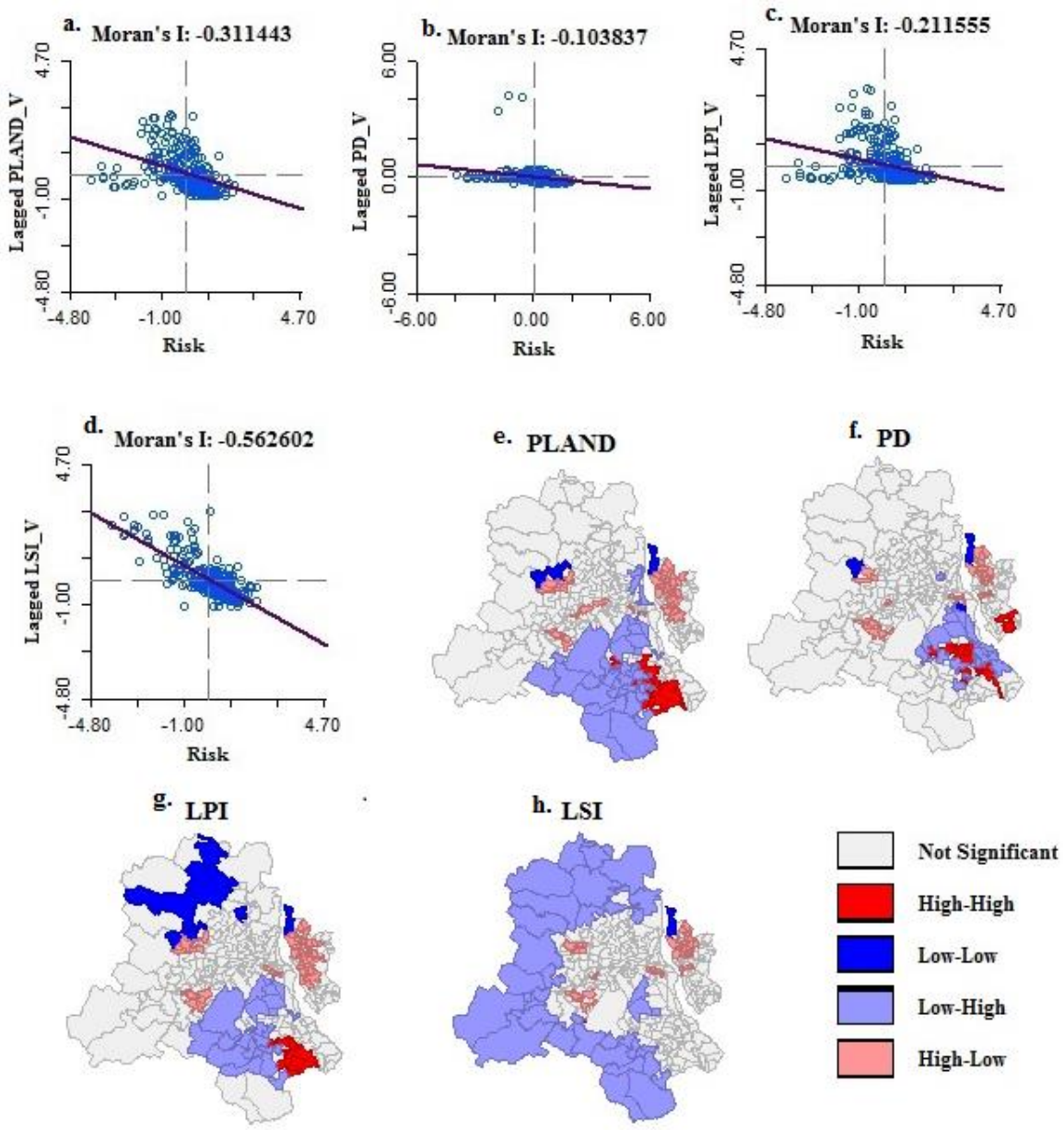

Fig. 8. Bi-variate Moran's I scatter plot between risk and green space form- a) risk vs. lagged PLAND; b) risk vs. lagged PD; c) risk vs. lagged LPI; d) risk vs. lagged LSI; and bi-variate LISA clustered map- e) risk vs. PLAND; f) risk vs. PD; g) risk vs, LPI; h) risk vs LSI.

4.3. Estimation of the influence of ULM on HRHR:

As we found significant auto-correlation between risk and ULM, thence to encounter it, spatial regression has been adopted. Initially, we normalized the data using *Z-score* statistics and removed multicollinearity effects using forward and backward multicollinearity test using

SPSS. Three variables, i.e., LPI_B, LSI_B, and PLAND_V, were excluded (Sup - 5) as VIF value was >6 and performed the OLS regression.

The result of the OLS model (Table 4) shows PLAND_B had a significant positive influence on stimulating the risk ($\beta = 0.60., \rho = 0.00$). But PD_B showed negative influence HRHR. That proved the dense and compacted built-up area is more prone to HRHR than low and medium dense built-up areas. Surprisingly, the regression coefficient for LPI_V showed a positive coefficient ($\beta = 0.22, \rho = 0.00$) with HRHR. The reasons may be due to all the large vegetation patches that were surrounded by the densely built-up area in Delhi. Since we had taken average summer night LST, hence, it can be said that larger vegetation patches surrounded by dense and compacted built-up may not be able to reduces risk significantly at night time. High R^2 value ($R^2 = 0.72$) and significant F value ($F=143.61; \rho = 0.00$) ensured efficiency of OLS model is acceptable. Though, Lagrange Multiplier (error) value of the model was found very high and significant ($LM\ error = 90.32; \rho = 0.00$) in diagnostics statistical table (Table 5). Which ensured error or residual terms are spatially auto-correlated, and estimated coefficient (β) may be biased. Thence, Spatial Error (SE) model adopted. The result from the SE model shows a similar trend, though values are slightly differing from the OLS model. For instance, the regression coefficient (β) of PLAND_B is 0.57 in the SE model and which was 0.61 in OLS. Overall model, performance has been significantly improved in the SE model as R^2 value increased to 0.80, and Akaike info criterion (AIC) value reduces from 450.92 in OLS to 385 in the SE model (Table 6). Besides, LISA clustered map of residual estimated by OLS and SE model and lower Moran's I in SE model than OLS indicates model performance has been better in SE (Fig. 9).

Table 4. The output from OLS and SE regression model.

Regression Model	Ordinary Least Square (OLS)		Spatial Error (SE)	
Variable	Coefficient (β)	Probability(ρ)	Coefficient(β)	Probability(ρ)
W_Risk	-----	--------	----	------
CONSTANT	0	0.99	-0.02	0.86
PLAND_B	0.61	0.00	0.57	0.00
PD_B	-0.10	0.05	-0.03	0.45
PD_V	-0.11	0.00	-0.09	0.00
LPI_V	0.22	0.00	0.10	0.04
LSI_V	-0.31	0.00	-0.31	0.00
LAMBDA	------	--------	0.66	0.00

Table 5. OLS model diagnostics statistics.

Diagnostic Statistics of OLS	MI/DF	VALUE	PROB
Moran's I	0.29	9.95	0
Lagrange Multiplier (lag)	1	50.02	0
Robust LM (lag)	1	3.54	0.05
Lagrange Multiplier (error)	1	90.32	0
Robust LM (error)	1	43.84	0
Lagrange Multiplier (SARMA)	2	93.86	0

Table 6. Comparison of model efficiency between OLS and SE model.

Criteria	OLS	Spatial Error
R-squared	0.72	0.80
F-statistic	143.61	--------
Log Likelihood	-219.46	-186.50
Akaike info criterion	450.92	385
Schwarx criterion	472.77	406.86
Standard error of regression	0.53	0.45

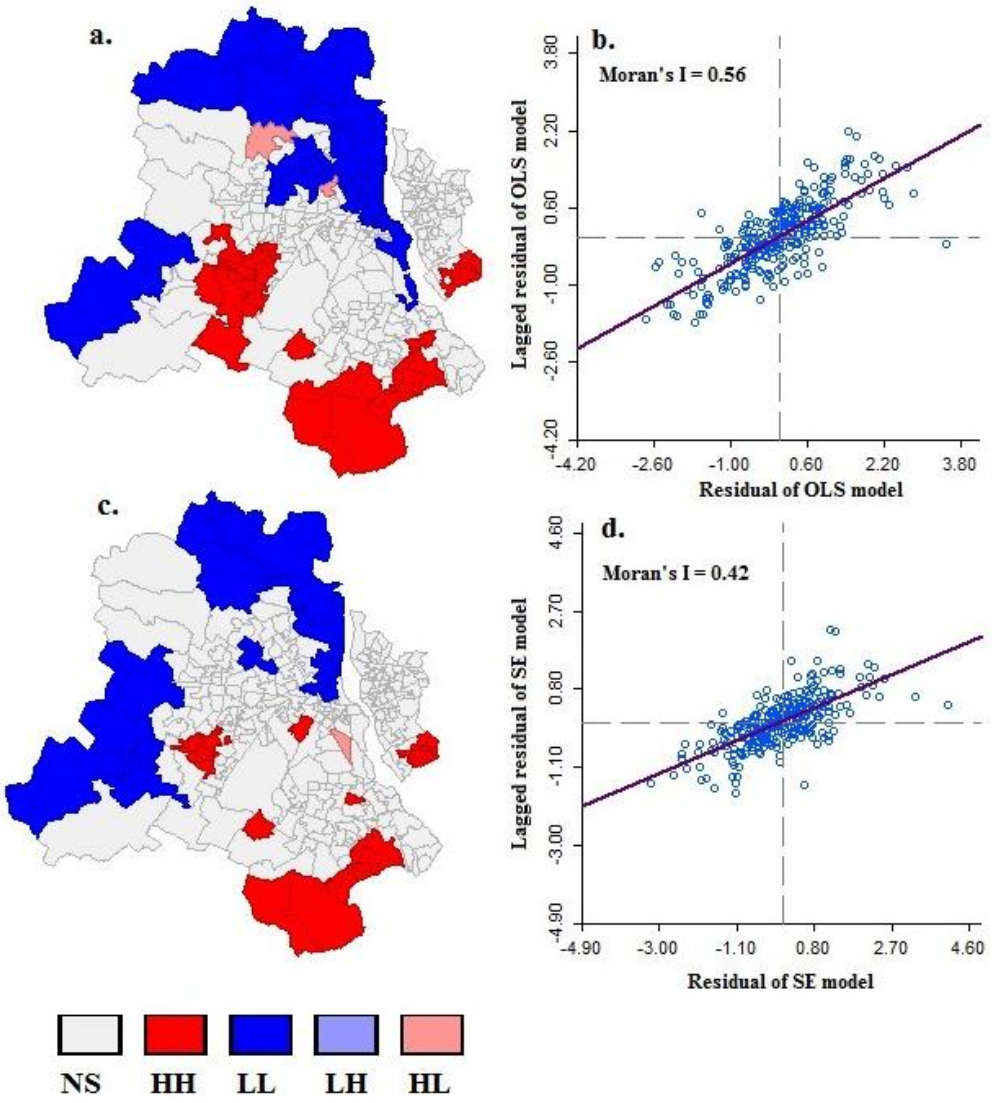

Fig. 9. Comparison of OLS and SE model in terms of LISA clustered map and Moran's I of residual terms from two models – a) LISA map of residual from the OLS model; b) Moran's I of residual from the OLS model; c) LISA map of residual from the SE model; b) Moran's I of residual from SE model

5. Validation:

Field observation pointed out that, level of awareness is quite low in very high and high HRHR zones, although they experienced health issues due to heat (Fig - 10). In the case of question no 1, for example, 64.3% of respondents in zone A were completely unknown about the temperature rising issue. However, it was inverse in zone C, where 86.4% of respondents were very much aware of the rise of temperature (Fig. 10). Most of the respondents in all these zones agreed that they had suffered from different health issues. These were respiratory,

cardiovascular problems, high blood pressure, skin problems due to fungal activity, headaches, shaking of hands and legs, irritation etc. due to severe heat during both day and night time. However, peoples were mainly belonged from the economically deprived sections of the society and also not concerned with either UHI or HRHR. Likewise, adaptive capacity was meager due to their low economic status. On the contrary, respondents from C (i.e., moderate and low-risk zones) were very much concerned about the UHI and its effects on health. They also faced similar kinds of health problems. Still, their adaptive capacity (i.e., availability of AC, cars with AC, refrigerator, water cooling facilities, etc.) was much better than people in very high and high-risk zones (source: open-ended discussion with respondents during field).

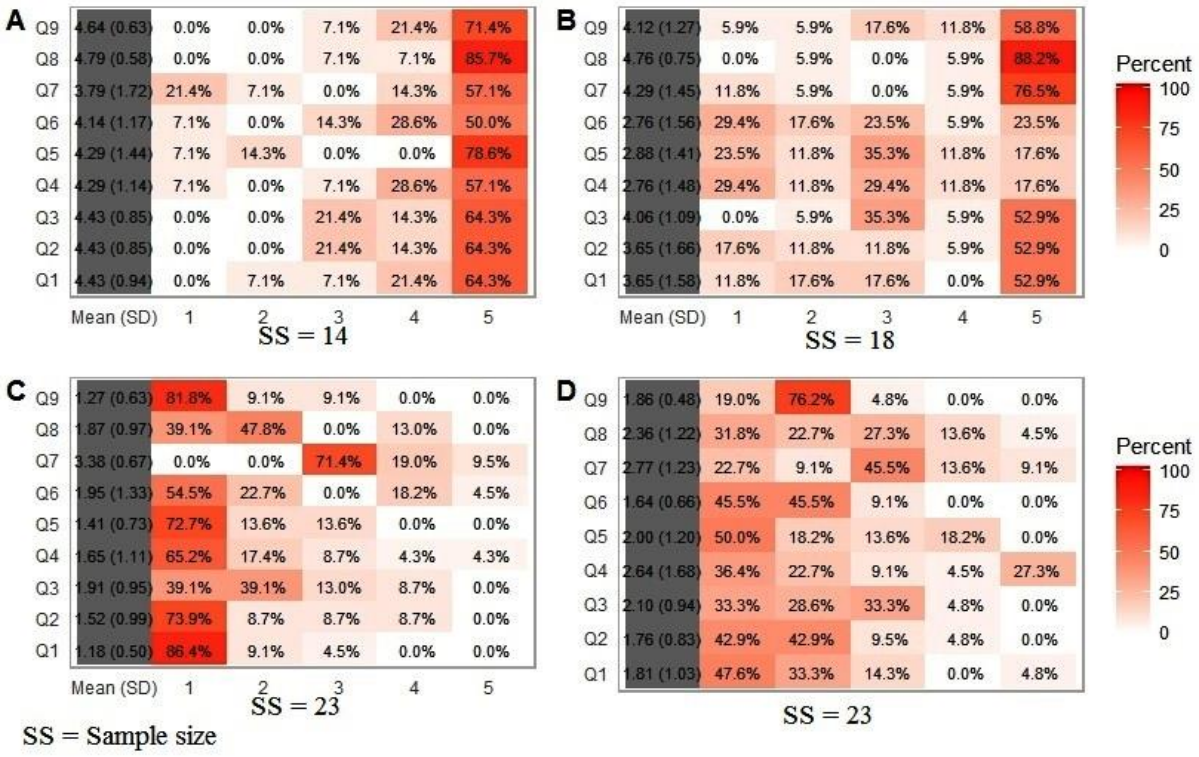

Fig. 10. Likert heat map representing zone wise people perception regarding UHI in Delhi.

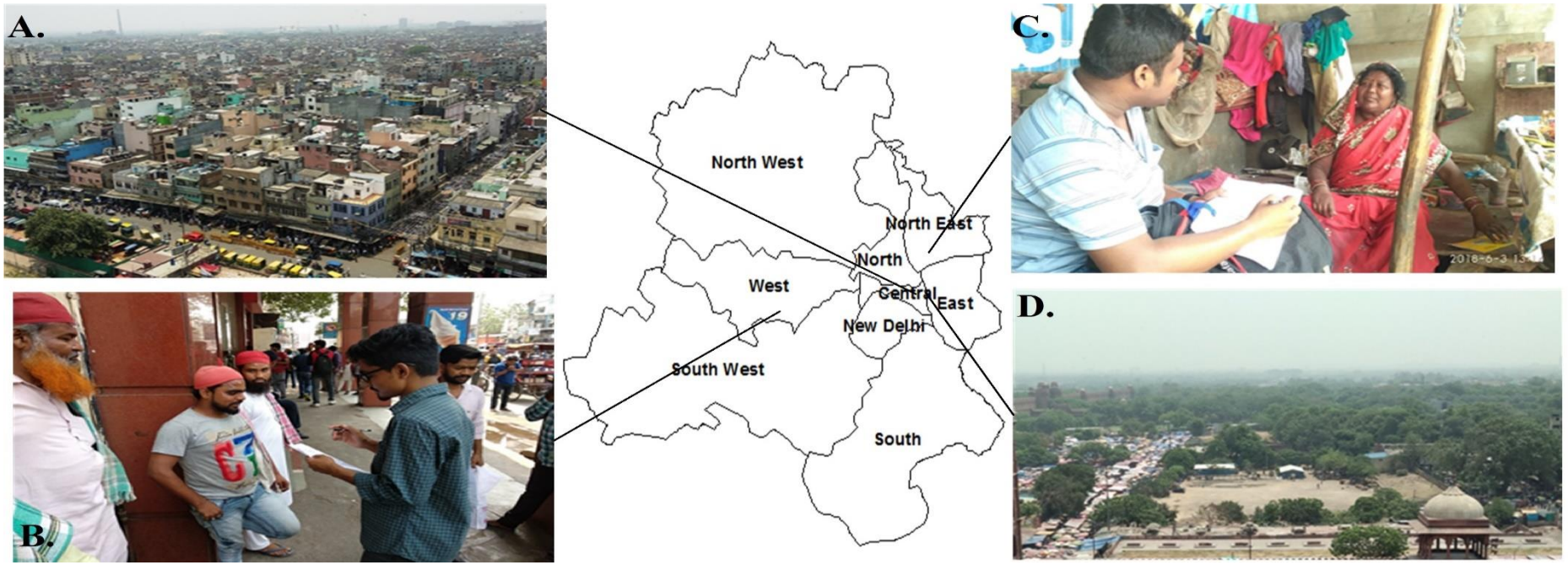

Fig. 11. Some snapshots from the field survey. A) dense urban landscape near Jamma Masjid in Old Delhi; conducting field survey B) near Uttam Nagar metro station in West Delhi; C) near Preet Vihar in East Delhi; D) abundance of urban green space near Red Fort in Central Delhi (Date of survey: April – June 2018).

6. Discussion and Conclusion:

6.1. Understanding the spatial pattern of HRHR in response to LULC in the city.

Risk assessment is essential for the implementations of heat resilience plans (Johnson et al., 2009; United Nations, 2015). As many cities around the world don't include where the most vulnerable sections of society have been residing in their planning procedure, hence people are suffering from the lack of proper emergency plans and strategy for HRHR mitigation. As Stone, (2009) mentioned that, sustainable urban planning undoubtedly lies in the proper LULC planning and implementation at the ground. Therefore, critical understandings related to health risk also holds the key to determinants for future LULC planning. Most of the cities around Global South faced a significant mismatch between city plan and ground reality. Delhi is not beyond these scenarios, as extensive migration, population growth continuously compelled to people to develop slum and *'jugghi jhopri'* and lived in environmentally critical zones (Singh and Grover, 2015). Which, in return, made them more vulnerable to extreme heat. In Delhi, high and very high risk not only concentrated in the central location (CL) but also formed some pockets in the NE, SE, and CW segments, which are highly populated and have highly dense built-up. NE and CL pockets are basically under the Old Delhi ('Purani Delhi,' i.e., Chadnichowk of Central Delhi, Shahdara, Preetvihar of NE Delhi) part, whereas CW is newly developed (Fig. 11). Undoubtedly these pockets are the prime concern for heat alert and heat mitigation activities. Apart from LULC changes, congestion, pollution, high built-up, and population density cumulatively altered the thermal profile of the city through increasing anthropogenic heat emission (Somvanshi, 2019).

In contrast, due to the presence of the many parks, street plants and other forms of greenery, the large part of Central region, located below the Old Delhi (i.e., New Delhi Municipal Council (NDMC), Delhi Cantonment Board (DCB)) was found at the medium and low-risk

zones. Abundance of urban greeneries due to strictly regulated land use change and planning by concern statutory body (i.e., NDMC & DCB) is responsible for that. In the NDMC most of the area used for the government and bureaucratic office where foreign embassy, Indian Parliament, Presidential Estate, etc. located, and in DCB, whole land use dedicated to defence purposes. Therefore, it is clearly evident that, controlling and regulating LULC in a proper way could create a local variation of thermal environment which ultimately influence HRHR and play an essential role in city sustainability. Now, the aforesaid argument probably seems very arbitrary if we can't provide strong empirical evidence. Hence there is need to linked LUM with HRHR quantitatively, which could have influence future LULC planning, discussed in section 6.2.

6.2. The synergy between ULM and HRHR:

There are some primary advantages of establishing a linkage between ULM and HRHR –

i. For identifying those locations where HRHR is making a clustered and outlier with ULM;
ii. To get the influence of ULM on HRHR;
iii. We can prevent other regions from entering high and very high-risk zones.

The strong positive spatial association between PLAND and LPI of built-up explains that high density and a continuous larger patch of built-up associated with high risk. It agrees with the existing literature where high risk has been identified in the highly-dense area of the city (Mushore et al., 2018; Zhang et al., 2019). Negative Moran's I value of vegetation configuration and composition again pinpoint the importance of the green space as a potential component of heat reduction effects. As we know, thick and larger vegetation patches are negatively associated with the HRHR due to having more evapotranspiration and more shading, so more cooling (Suvamoy Pramanik and Punia, 2019). In contrast, fragmented green spaces

don't have similar cooling efficiency hence high risk. This direct linkage of ULM with HRHR can enhance our understandings of LST – LULC and risk spectra as well as identified the clustered where need urgent attention.

Now the point is how this result can contribute to building a heat resilience city, which can be traced from the result of regression models. PLAND_B is found as the main contribution of risk, whereas the negative coefficient of PD_B indicates fragmentation leads to less HRHR. Our observation found that urban density has a strong contribution towards creating high HRHR. The mechanism is very clear, as materials which are used to build impervious surface have high heat absorption capacity, heat has been captured at the day time and release in the night (Stone et al., 2010). Besides, 'heat-trapping' effects by 'urban canyon' also contribute significantly (Oke, 2011) and cumulatively alter the thermal profile local ambient. The most important finding is that positive coefficient (β) of LPI_V with Risk, indicated despite high cooling efficiency during day time (Suvamoy Pramanik and Punia, 2019). It depicted that the larger patch of vegetation, surrounded by the dense built-up, might not have similar cooling capacity during summer season night. Contrastingly, negative coefficient (β) PD_V indicated that medium dense built-up with the abundance of vegetation patch would be a targeted land use plan for the rest of the regions of Delhi.

6.3. Policy lag:

Indian cities are substantially suffering from the lack of heat mitigation plans (Chaudhary, 2018). Despite several studies (Bhati and Mohan, 2016; Mohan and Kandya, 2015) identified numbers of UHI pockets, and the local government pays little attention. Recent statistics showed that between 2005 and February 2018, the government allowed the cutting of 112169 trees in the name of development (Singh, 2019). Moreover, the recent initiative taken by the local government, to cutting down of more than 15000 trees for the development of

seven residential colonies is very surprising and upsetting (Menon and Kohli, 2017). As we concern that, for long term solutions for not only heat reduction but also for other environmental issues, urban greeneries are the only option. However, Delhi Government drafted 'tree relocation scheme' for translocating healthy trees which will be cut due to construction, is not realistic and less cost-effective (Nandi, 2018). We argued there should be heat mitigation plan which could coordinate all the concerned authorities and deal with all possible aspects comprehensively. Meanwhile, lessons from the Ahmedabad Heat Action Plan (HAP, i.e., using high reflective materials on the rooftop, coloring, and gardening the roof, affordable rooftop covering with jute bags, use of green netting, etc. could be important learning for Delhi (Ahmedabad Municipal Corporation, 2013). Besides, the lack of people awareness about UHI, as reflected in the field survey, needs to be considered as a serious matter. From our observation, we could suggest some inputs which could be an essential part of effective heat mitigation plan –

i. Those pockets which are identified as high and very high risk needs some immediate action.
ii. The regions where rapid urbanization happening (Jain et al., 2019) should be brings under controlled and regulated growth scenarios. So, we can stop these regions from becoming a future high HRHR zone.
iii. Medium dense with abundant vegetation may be the alternative option for future land use.
iv. There is the urgent need of public awareness-raising campaigns, strengthen early warning system and forecasting, incorporation of social media and mass media for knowledge improvement and color based warning system.
v. Last but not least, we have to secure urban greeneries for our better and sustainable future.

6.5. Conclusion:

Heatwave and UHI are now becoming a global phenomenon and can happen in any community. Meanwhile, uncertain climatic behavior making it highly unpredictable also. Therefore, the pre-identification of the risk-prone areas always makes sense. This study combines pre-existing knowledge, methods, and added spatial metrics of LULC with risk through spatial statistics in a very dense city among developing countries, i.e., Delhi. The result of the study not only identified most risk-prone areas but also provides local guidance to the planners for resource allocation and mobilization. It may be suggested that medium dense built-up with proper green space would be the ideal LULC planning for reducing the HRHR. Though further works need with combination of large numbers of downscaled data to explore another possible dimension of risk assessment.

Author's Contribution:

SP conceptualized and conducted the research. SP also wrote the initial draft of the manuscript. MP and SC checked the initial draft, and SP corrected. Finally, all are reviewed the manuscript.

Acknowledgment:

This research was part of M.Phil. Dissertation submitted by SP at CSRD, SSS, Jawaharlal Nehru University, New Delhi. It is solely an academic work. The authors would like to acknowledge Mr. Malay Kotal for assistance during the field survey and Dr. Biswajit Mondal for his valuable comments on the manuscripts.

Financial Support:

SP would like to acknowledge the University Grants Commission – Junior Research Fellowship (UGC-JRF) for financial support during research work.

Declaration:

The authors reported no potential conflict of interest.

References:

Ahmedabad Municipal Corporation, 2013. Ahmedabad Heat Action Plan 1–24. https://doi.org/10.1371/journal.pone.0091831

Anselin, L., Syabri, I., Kho, Y., 2006. GeoDa: An introduction to spatial data analysis. Geogr. Anal. https://doi.org/10.1111/j.0016-7363.2005.00671.x

Azhar, G., Saha, S., Ganguly, P., Mavalankar, D., Madrigano, J., 2017. Heat wave vulnerability mapping for India. Int. J. Environ. Res. Public Health 14, 357.

Bhati, S., Mohan, M., 2016. WRF model evaluation for the urban heat island assessment under varying land use/land cover and reference site conditions. Theor. Appl. Climatol. 126, 385–400. https://doi.org/10.1007/s00704-015-1589-5

Buscail, C., Upegui, E., Viel, J.-F., 2012. Mapping heatwave health risk at the community level for public health action. Int. J. Health Geogr. 11, 38.

Chakraborti, S., Banerjee, A., Sannigrahi, S., Pramanik, S., Maiti, A., Jha, S., 2019. Assessing the dynamic relationship among land use pattern and land surface temperature: A spatial regression approach. Asian Geogr. 1–24.

Chakraborty, T., Lee, X., 2019. A simplified urban-extent algorithm to characterize surface urban heat islands on a global scale and examine vegetation control on their spatiotemporal variability. Int. J. Appl. Earth Obs. Geoinf. 74, 269–280. https://doi.org/10.1016/J.JAG.2018.09.015

Chaudhary, J., 2018. India needs strategies to combat urban heat stress. India Clim. Dialouge.

Chen, X.L., Zhao, H.M., Li, P.X., Yin, Z.Y., 2006. Remote sensing image-based analysis of the relationship between urban heat island and land use/cover changes. Remote Sens. Environ. 104, 133–146. https://doi.org/10.1016/j.rse.2005.11.016

CIESIN - Center for International Earth Science Information Network - - Columbia University, 2018. Gridded Population of the World, Version 4 (GPWv4): Basic Demographic Characteristics, Revision 11.

Crichton, D., 1999. The risk triangle. Nat. disaster Manag. 102–103.

Cunningham, A., 2018. Are we ready for the deadly heat waves of the future? Sci. News 18.

Curriero, F.C., Heiner, K.S., Samet, J.M., Zeger, S.L., Strug, L., Patz, J.A., 2002. Temperature and mortality in 11 cities of the eastern United States. Am. J. Epidemiol. 155, 80–87.

Cutter, S.L., Boruff, B.J., Shirley, W.L., 2003. Social vulnerability to environmental hazards. Soc. Sci. Q. 84, 242–261.

Doxsey-Whitfield, E., MacManus, K., Adamo, S.B., Pistolesi, L., Squires, J., Borkovska, O., Baptista, S.R., 2015. Taking advantage of the improved availability of census data: a first look at the gridded population of the world, version 4. Pap. Appl. Geogr. 1, 226–234.

Du, S., Xiong, Z., Wang, Y.C., Guo, L., 2016. Quantifying the multilevel effects of landscape composition and configuration on land surface temperature. Remote Sens. Environ. 178, 84–92. https://doi.org/10.1016/j.rse.2016.02.063

Estoque, R.C., Ooba, M., Seposo, X.T., Togawa, T., Hijioka, Y., Takahashi, K., Nakamura, S., 2020. Heat health risk assessment in Philippine cities using remotely sensed data and social-ecological indicators. Nat. Commun. 1–12. https://doi.org/10.1038/s41467-020-15218-8

Fouillet, A., Rey, G., Laurent, F., Pavillon, G., Bellec, S., Ghihenneuc-jouyaux, C., Clavel, J., Jougla, E., Hémon, D., 2006. Excess mortality related to the August 2003 heat wave in France. Int Arch Occup Env. Heal. 80, 16–24.

Gabriel, K.M.A., Endlicher, W.R., 2011. Urban and rural mortality rates during heat waves in Berlin and Brandenburg, Germany. Environ. Pollut. 159, 2044–2050. https://doi.org/10.1016/j.envpol.2011.01.016

Garssen, J., Harmsen, C., de Beer, J., 2005. The effect of the summer 2003 heat wave on mortality in the Netherlands. Euro Surveill. Bull. Eur. sur les Mal. Transm. = Eur. Commun. Dis. Bull. 10, 165–168. https://doi.org/557 [pii]

Government of India, 2011. Census of India 2011. State Lit. 3–4. https://doi.org/10.2105/AJPH.2010.193276

Hajat, S., Armstrong, B.G., Gouveia, N., Wilkinson, P., 2005. Mortality displacement of heat-related deaths: a comparison of Delhi, Sao Paulo, and London. Epidemiology 16, 613–620.

Harlan, S.L., Brazel, A.J., Prashad, L., Stefanov, W.L., Larsen, L., 2006. Neighborhood microclimates and vulnerability to heat stress. Soc. Sci. Med. 63, 2847–2863. https://doi.org/10.1016/j.socscimed.2006.07.030

Jain, M., Korzhenevych, A., Sridharan, N., 2019. Determinants of growth in non-municipal areas of Delhi: rural--urban dichotomy revisited. J. Hous. Built Environ. https://doi.org/10.1007/s10901-019-09655-1

Johnson, D.P., Stanforth, A., Lulla, V., Luber, G., 2012. Developing an applied extreme heat vulnerability index utilizing socioeconomic and environmental data. Appl. Geogr. 35, 23–31. https://doi.org/10.1016/j.apgeog.2012.04.006

Johnson, D.P., Wilson, J.S., Luber, G.C., 2009. Socioeconomic indicators of heat-related health risk supplemented with remotely sensed data. Int. J. Health Geogr. 8, 57. https://doi.org/10.1186/1476-072X-8-57

Kumari, S., Punia, M., 2017. Social Vulnerability Mapping for Delhi BT - Marginalization in Globalizing Delhi: Issues of Land, Livelihoods and Health, in: Acharya, S.S., Sen, S., Punia, M., Reddy, S. (Eds.), . Springer India, New Delhi, pp. 253–270. https://doi.org/10.1007/978-81-322-3583-5_14

Li, J., Song, C., Cao, L., Zhu, F., Meng, X., Wu, J., 2011. Impacts of landscape structure on surface urban heat islands: A case study of Shanghai, China. Remote Sens. Environ. 115, 3249–3263. https://doi.org/10.1016/j.rse.2011.07.008

Lindley, S.J., Handley, J.F., McEvoy, D., Peet, E., Theuray, N., 2007. The role of spatial risk assessment in the context of planning for adaptation in UK urban areas. Built Environ. 33, 46–69.

Mallick, J., Rahman, A., 2012. Impact of population density on the surface temperature and micro-climate of Delhi. Curr. Sci. 102, 1708–1713.

Mavalankar, D., Shah Azhar, G., Sarma, A., Rajiva, A., Thube, N., Dholakia, H., Hess, J., Van Tran, K., Sheffield, P., Jaiswal, A., Knowlton, K., Khosla, R., Connolly, M., Deol, B., Casey-Lefkowitz, S., Gill, G., 2013. Rising Temperature, Deadlu Threat: Recommendations for Health Professionals in Ahmedabad. Nat. Resour. Def. Counc.

Mcgarigal, K.S.K.E.E., 2012. FRAGSTATS v4: Spatial Pattern Analysis Program for Categorical and Continuous Maps.

Menon, M., Kohli, K., 2017. Saving Delhi's trees [WWW Document]. The Hindu.

Mohammad, P., Goswami, A., Bonafoni, S., 2019. The impact of the land cover dynamics on surface urban heat island variations in semi-arid cities: A case study in Ahmedabad City, India, using multi-sensor/source data. Sensors (Switzerland) 19. https://doi.org/10.3390/s19173701

Mohan, M., Kandya, A., 2015. Impact of urbanization and land-use/land-cover change on diurnal

temperature range: A case study of tropical urban airshed of India using remote sensing data. Sci. Total Environ. 506–507, 453–465. https://doi.org/10.1016/j.scitotenv.2014.11.006

Moran, P.A.P., 1950. Notes on continuous stochastic phenomena. Biometrika 37, 17–23.

Mushore, T.D., Mutanga, O., Odindi, J., Dube, T., 2018. Determining extreme heat vulnerability of Harare Metropolitan City using multispectral remote sensing and socio-economic data. J. Spat. Sci. 63, 173–191. https://doi.org/10.1080/14498596.2017.1290558

Nandi, J., 2018. Transplanting no alternative as most trees don't survive it. Times of India.

Nations, U., 2018. World Urbanization Prospects, Demographic Research. https://doi.org/10.4054/demres.2005.12.9

O'Neill, M.S., Zanobetti, A., Schwartz, J., 2003. Modifiers of the temperature and mortality association in seven US cities. Am. J. Epidemiol. 157, 1074–1082.

Oda, T., Maksyutov, S., Andres, R.J., 2018. The Open-source Data Inventory for Anthropogenic CO 2, version 2016 (ODIAC2016): a global monthly fossil fuel CO 2 gridded emissions data product for tracer transport simulations and surface flux inversions. Earth Syst. Sci. Data 10, 87–107.

Oke, T.R., 2011. Urban heat island, in: The Routledge Handbook of Urban Ecology. Routledge Abingdon, Oxon, pp. 120–131.

Patz, J.A., Campbell-Lendrum, D., Holloway, T., Foley, J.A., 2005. Impact of regional climate change on human health. Nature 438, 310.

Pramanik, Suvamoy, Punia, M., 2019. Assessment of green space cooling effects in dense urban landscape: a case study of Delhi, India. Model. Earth Syst. Environ. 5, 867–884. https://doi.org/10.1007/s40808-019-00573-3

Pramanik, S., Punia, M., 2019. Land use/land cover change and surface urban heat island intensity: source–sink landscape-based study in Delhi, India. Environ. Dev. Sustain. https://doi.org/10.1007/s10668-019-00515-0

PTI, 2015. No fresh heatwave deaths as rains hit Andhra Pradesh, Telangana [WWW Document]. Firstpost.

Reid, C.E., Mann, J.K., Alfasso, R., English, P.B., King, G.C., Lincoln, R.A., Margolis, H.G., Rubado, D.J., Sabato, J.E., West, N.L., 2012. Evaluation of a heat vulnerability index on abnormally hot days: an environmental public health tracking study. Environ. Health Perspect. 120, 715–720.

Rooney, C., McMichael, A.J., Kovats, R.S., Coleman, M.P., 1998. Excess mortality in England and Wales, and in Greater London, during the 1995 heatwave. J. Epidemiol. Comm. Hlth. 52, 482–486.

Singh, R.., Grover, A., 2015. Sustainable Urban Environment in Delhi Mega City: Emerging Problems and Prospects for Innovative Solutions. Br. GSDR 2.

Singh, S., 2019. For Delhi to survive, its trees must breathe free. Hindusthantimes.

Somvanshi, A., 2019. Indian cities are simmering in their own waste heat [WWW Document]. Down To Earth.

Stone, B., 2009. Land Use as Climate Change Mitigation. Environ. Sci. Technol. 43, 9052–9056. https://doi.org/10.1021/es902150g

Stone, B., Hess, J.J., Frumkin, H., 2010. Urban form and extreme heat events: Are sprawling cities more vulnerable to climate change than compact cities? Environ. Health Perspect. 118, 1425–

1428. https://doi.org/10.1289/ehp.0901879

Sultana, S., Satyanarayana, A.N.V., 2018. Urban heat island intensity during winter over metropolitan cities of India using remote-sensing techniques: impact of urbanization. Int. J. Remote Sens. 39, 6692–6730. https://doi.org/10.1080/01431161.2018.1466072

Thakur, J., 2017. Heatwave to intensify in Delhi, mercury to touch 43 degrees by Monday. Hindusthantimes.

The Guardian, 2016. Rain brings little relief to southern India as heatwave death toll nears 2,200. Guard.

Tomlinson, C.J., Chapman, L., Thornes, J.E., Baker, C.J., 2011. Including the urban heat island in spatial heat health risk assessment strategies: a case study for Birmingham, UK. Int. J. Health Geogr. 10, 42. https://doi.org/10.1186/1476-072X-10-42

United Nations, 2015. Sendai Framework for Disaster Risk Reduction 2015 - 2030.

Vandentorren, S., Bretin, P., Zeghnoun, A., Mandereau-Bruno, L., Croisier, A., Cochet, C., Ribéron, J., Siberan, I., Declercq, B., Ledrans, M., 2006. August 2003 heat wave in France: risk factors for death of elderly people living at home. Eur. J. Public Health 16, 583–591.

Vyas, A., Shastri, B., Joshi, Y., 2014. Spatio-temporal analysis of UHI using geo-spatial techniques: A case study of Ahmedabad city. Int. Arch. Photogramm. Remote Sens. Spat. Inf. Sci. - ISPRS Arch. 40, 997–1002. https://doi.org/10.5194/isprsarchives-XL-8-997-2014

Wang, J., Kuffer, M., Sliuzas, R., Kohli, D., 2019. The exposure of slums to high temperature: Morphology-based local scale thermal patterns. Sci. Total Environ. 650, 1805–1817.

WHO, 2018. Information and public health advice: heat and health. World Heal. Organ.

Yaron, M., Niermeyer, S., 2004. Clinical description of heat illness in children, Melbourne, Australia—a commentary. Wilderness Environ. Med. 15, 291–292.

Yu, Z., Yang, G., Zuo, S., Jørgensen, G., Koga, M., Vejre, H., 2020. Critical review on the cooling effect of urban blue-green space: A threshold-size perspective. Urban For. Urban Green. https://doi.org/10.1016/j.ufug.2020.126630

Yue, W., Liu, X., Zhou, Y., Liu, Y., 2019. Impacts of urban configuration on urban heat island: An empirical study in China mega-cities. Sci. Total Environ. 671, 1036–1046. https://doi.org/10.1016/j.scitotenv.2019.03.421

Zhang, W., Zheng, C., Chen, F., 2019. Mapping heat-related health risks of elderly citizens in mountainous area: A case study of Chongqing, China. Sci. Total Environ. 663, 852–866.

Zhou, G., Wang, H., Chen, W., Zhang, G., Luo, Q., Jia, B., 2020. Impacts of Urban land surface temperature on tract landscape pattern, physical and social variables. Int. J. Remote Sens. 41, 683–703. https://doi.org/10.1080/01431161.2019.1646939

Zhou, W., Cao, F., 2020. Effects of changing spatial extent on the relationship between urban forest patterns and land surface temperature. Ecol. Indic. 109, 105778. https://doi.org/10.1016/j.ecolind.2019.105778

Zhou, W., Huang, G., Cadenasso, M.L., 2011. Does spatial configuration matter? Understanding the effects of land cover pattern on land surface temperature in urban landscapes. Landsc. Urban Plan. 102, 54–63. https://doi.org/10.1016/j.landurbplan.2011.03.009